Int. J. Electrochem. Sci., 7 **(2012)** 9537 - 9549

International Journal of
ELECTROCHEMICAL
SCIENCE
www.electrochemsci.org

Synthesis and Characterization of Carbon Nanospheres from Hydrocarbon Soot

Anu.N.Mohan, B. Manoj[*]

Department of Physics, Christ University, Bangalore, Karnataka, India, 560029
[*]E-mail: manoj.b@christuniversity

Received: 10 August 2012 / *Accepted:* 15 September 2012 / *Published:* 1 October 2012

Foreseeing the upcoming era of the carbon nanomaterials and their revolutionary applications, we have identified and explored the structural parameters of five effective precursors of the same -carbon black, soot obtained by the thermal decomposition of kerosene, diesel, paraffin wax and lubricant oil. Micro-Raman spectroscopy, Fourier Transform Infrared Spectroscopy (FT-IR), X-ray diffraction (XRD), Scanning Electron Microscopy, Electron dispersive spectroscopy (EDS) and elemental analysis are employed for the structural and morphological characterization of the nanomaterials formed. The average lateral size (L_a), stacking height (L_c) and interlayer spacing (d_{002}) of the crystallite structures calculated from the X-ray intensities are found to be ranging from 4.3-5.9 nm, 0.63-2.40 nm and 3.10- 3.68 Å respectively. L_a values determined by Raman and XRD analysis are in very good agreement thereby reinforcing the nanocrystalline structure of the samples. The very low I_{20}/I_{26} ratio obtained reveals a relatively low amount of disorder in the nanostructures. Nanomaterials formed have the morphology of non-uniform nanospheres with diameter varying between 26-100 nm. EDS and elemental analysis confirms the absence of metal impurities. FTIR spectra of the samples shows the presence of stretching vibrations of –OH bonds, aliphatic –CH, $–CH_2$ and $–CH_3$ absorptions, C=C and –CH absorptions of aromatic structures.

Keywords: Carbon nanosphere, nanocrystalline structure, microraman spectroscopy

1. INTRODUCTION

Carbon nanotubes (CNTs) and nanostructures were one of the blooming fields of research from the early half of the 19th century and have been in constant limelight since then. They have been extensively researched in the past few years and are ranked as one of the most exciting scientific development of the period [1-2]. The immense research interest in this field is primarily driven by the unique physical and chemical properties of carbon nanomaterials, making it suitable for a whole host of applications ranging from clean energy to nano scale electronics to neuro-protective agents.

However, the problem of high production cost, caught up with the glory of carbon nanomaterials and hence it is highly desirable to synthesize well-ordered and well densed arrays of purified CNT at relatively simple, low cost and scalable technique. Purified petroleum products such as methane, benzene, acetylene etc are currently in practice for synthesizing CNTs. However, in view of the foreseen crisis of fossil fuels and increasing environmental pollution, researchers are looking for alternative sources for the production of nanomaterials. Diesel, Kerosene and Paraffin wax have been used as a precursor to produce carbon nanomaterial without a catalyst precursor[3-4]. Kerosene and diesel are complex mixture of aromatic and aliphatic hydrocarbon with carbon numbers predominantly in the C_9-C_{16} and C_9-C_{23} range, with most of these compounds being members of the paraffinic, napthenic or aromatic group of hydrocarbons. Paraffin wax is made of solid hydrocarbon with carbon numbers ranging from C_{20}-C_{40}[1-6]. Another important and less investigated potential source for carbon nanomaterials are soot obtained from the thermal decomposition of lubricants or motor oil and carbon black which is virtually pure elemental carbon in the form of colloidal particles that are produced by incomplete combustion or thermal decomposition of gaseous or liquid hydrocarbons under controlled conditions.

In the study presented here, carbon black and the soot obtained by the pyrolysis of commercially available kerosene, diesel oil, paraffin wax and lubricant oil are investigated. The structural and morphological features of the various samples are analysed by Micro-Raman Spectroscopy, Fourier Transform Infrared (FT-IR) Spectroscopy, Scanning Electron Microscope (SEM), Energy dispersive Spectroscopy (EDS), X-Ray Diffraction (XRD) and CHNS analysis.

2. EXPERIMENTAL DETAILS

2.1. Preparation of samples

Commercially available kerosene, diesel and lubricant oil (Mac multigrade engine oil for petrol cars) without any further purification were selected for this study. Kerosene, diesel and lubricant oil were placed in three separate simple laboratory lamps with a combustible cylindrical cotton material and the lamp was left for about 24 hours to absorb the respective samples. The lamps were lighted and allowed to burn in open air. Clean, flat ceramic tiles were placed above the flame of the lamps in order to collect the soot emitted from the lamps. When a sufficient amount of soot was collected, the experiments were terminated and the samples were allowed to dry. Paraffin wax soot was obtained by burning commercially available paraffin wax candles in open air. The soot emitted is collected by placing a ceramic tile horizontally above the flame. Carbon Black is obtained from a tyre factory and the sample is grounded to a fine powder. The Samples thus prepared are then subjected to various analytical techniques.

2.2.Raman spectroscopy analysis

Raman scattering measurements were recoreded at room temperature using Horiba Jobin Yvon Lab Ram HR system at a spatial resolution of 2 mm in the backscattering configuration. The 514 nm

line of He Ne laser with a power of 1.20 mW was used for excitation. The samples were scanned between 100- 4000 cm^{-1}, with a data acqusition time of 20s. For all the spectra, a linear baseline correction was used and the peak analysis was performed with Origin lab- 8.0 software. The planar microcrystalline size (L_a) for the sample was calculated from the intensities of D and G bands on the Raman spectra using Tuinstra and Koening (T-K) relation (Equn.1).

$$L_a = 4.35 (I_G/I_D) \text{ nm} \ldots\ldots\ldots\ldots\ldots\ldots\ldots\ldots\ldots\ldots\ldots\ldots (1)$$

2.3. X-ray diffraction analysis

The XRD data collection was performed by a Bruker AXS D8 Adance X-ray diffractometer at SAIF, Cochin University. Powdered samples were scanned from 5-70^o in 2 theta range with 0.03^o step interval and 2s/step counter time. Origin lab- 8.0 software was used for deconvolution of the diffractogram in the 2 theta region of 18-32^o.

The lateral size (L_a) and stacking height (L_c) of the crystallites were determined using the Scherrer equations (Equns.2 and 3).

$$L_a = 1.84 \lambda / B_a \text{ Cos}(\phi_a) \ldots\ldots\ldots\ldots\ldots\ldots\ldots\ldots\ldots\ldots\ldots\ldots (2)$$

$$L_c = 0.89 \lambda / B_c \text{ Cos}(\phi_c) \ldots\ldots\ldots\ldots\ldots\ldots\ldots\ldots\ldots\ldots\ldots\ldots (3)$$

where λ was the wavelength of the radiation used, B_a and B_c were the width of the (100) and (002) peaks respectively at 50% height, and ϕ_a and ϕ_c were the corresponding angles or peak positions [5-8].

2.4. FTIR spectroscopy analysis

The FTIR spectra of the soot samples were recorded over the range 4000- 500 cm^{-1} on a Shimadzu FTIR-8400 spectrometer using the KBr pellet technique. The total number of scans were 50 with a spectral resolution of 4 cm^{-1}.

2.5. SEM-EDS analysis

SEM micrographs and EDS measurements were obtained using Model JSM 6390 from JOEL Company, Japan.

2.6. Elemental analysis

The elemental analysis of the samples was carried out using the Vario EL III CHNS analyser.

3. RESULTS AND DISCUSSION

3.1. X-ray diffraction

The comparative study of the XRD profiles of all the five samples along with that of pure graphite is presented in Fig.1. All the samples show two distinct peaks at ~25^o of higher intensity and a slightly broadened peak around 42^o. The prominent (002) peak at ~25^o is assigned to the graphitic carbon in the sample. This peak located at 2θ angle of ~42.33^o can be readily assigned to (100) diffraction of graphene and is a signature of the hexagonal graphite lattice of multi-walled CNTs present.

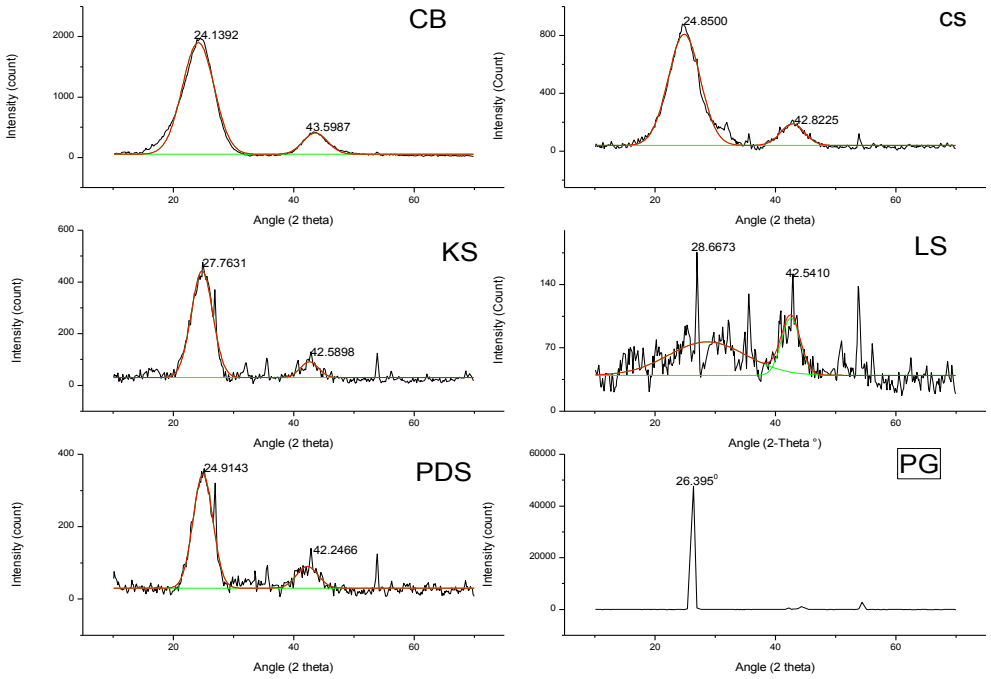

Figure 1. XRD spectra of soot obtained from the atmospheric pyrolysis of carbon black (CB), paraffin wax (CS), kerosene (KS), lubricant (LS), Diesel (PDS) and graphite (PG)

The presence of strong and broadened π band in all the samples suggests that the carbon nanospheres (CNSs) formed is composed more of crystalline graphitic carbon. The γ-band at ~20^o originates from the disorder in the sp^2 hybridized carbon and indicates lattice disorder in the curved graphene sheets, spheres, tube ends etc[8-11]. A comparatively low intensity of the γ-band in the XRD profile of the samples indicates that all the nanomaterials synthesized have a very low percentage of disordered amorphous carbon while the appearance of the high intensity π band in all of them shows that the samples have a high degree of crystallinity or graphitization. The disordered carbon are composed of both sp^3 and sp^2 sites. The sp^3 sites have only σ states whereas the sp^2 sites also possess π states. π states are different, because a π orbital usually interacts with π states of more than one atom

to form a conjugated system such as in benzene. The medium-range order due to π-bonding distinguishes disordered carbons from the σ-bonded amorphous carbon. π-bonding is maximized if the π states form pairs of aligned π-states, or six fold aromatic rings or graphitic clusters of aromatic rings. This usually occurs in graphitic carbon with microcrystalline structure [1-7].

Relative intensity of γ (or I_D) and π (or I_G) peaks- (I_D/I_G) ratio- is a direct measure of the amount of disorder in the crystallinity and is observed to be in between 1.1 to 0.07. Prefereably, for nanocrystalline carbon, this value is sought to be as low as possible [1]. I_D/I_G ratio reported by the previous studies on CNTs produced by various techniques is between 0.5 to 1.3. The intensity ratio for the samples we investigated is much lower than the reported value of CNTs obtained by thermal decomposition (Table.1). The dimensions of the graphite domains present in the samples are also characterized by the average stacking height of the parallel layers in the 'c' direction (L_c) and average diameter of the parallel layers in the 'ab' plane (L_a). The lateral size of the aromatic lamina (L_a) formed is found to be ranging from 4.3-5.9 nm where as stacking height (L_c) is found to be varying from 0.63-2.40 nm. The interlayer spacing (d_{002}) of graphite and semi-graphite normally lies within a value of 3.54-3.37 Å. The d_{002} value of the lamellae in the samples is found to be ranging from 3.10-3.68 Å, which is near to the value of graphite layer reported in various studies.

Table 1. Structural parameters and elemental composition of CNS synthesized

Sample	G band 2θ degree	Ratio I_D/I_G	d_{002} Å	L_c Å	L_a Å	N	n	C %	H %	H/C
KS	24.7	0.13	3.59	22.64	47.93	7	17	99.21	0.69	0.007
CS	24.8	0.22	3.57	15.12	44.30	5	9	96.31	1.12	0.013
PDS	24.9	0.07	3.58	24.44	59.02	8	20	97.17	0.88	0.009
LS	28.6	1.18	3.10	06.33	45.52	3	3	97.4	0.53	0.005
CB	24.1	0.43	3.68	15.27	43.23	5	8	97.87	0.00	0.000

(d_{002}-interlayer spacing; L_c-stacking height; L_a-lateral size of the aromatic lamallae; N-number of aromatic lamallae; n- average number of carbon atoms per lamellae; C-carbon wt %; H-hydrogen wt %; H/C-ratio of hydrogen to carbon wt %)

3.2. SEM-EDS analysis

The HR-SEM micrograph of the carbon nanomaterial formed by the pyrolysis of kerosene is presented in Fig.2.a. The surface morphology of the soot deposited appears to be non-uniform nanospheres. The particle diameter under a 100,000 magnification is observed as 62.48-108.41nm.

The EDS data of the soot is also presented in Fig.2.a. The spectrum shows the presence of carbon and oxygen as the thermolytic byproduct of kerosene. The EDS analysis indicates that the soot consists of about 99.21% weight of carbon and 0.79% weight of oxygen without any other impurity.

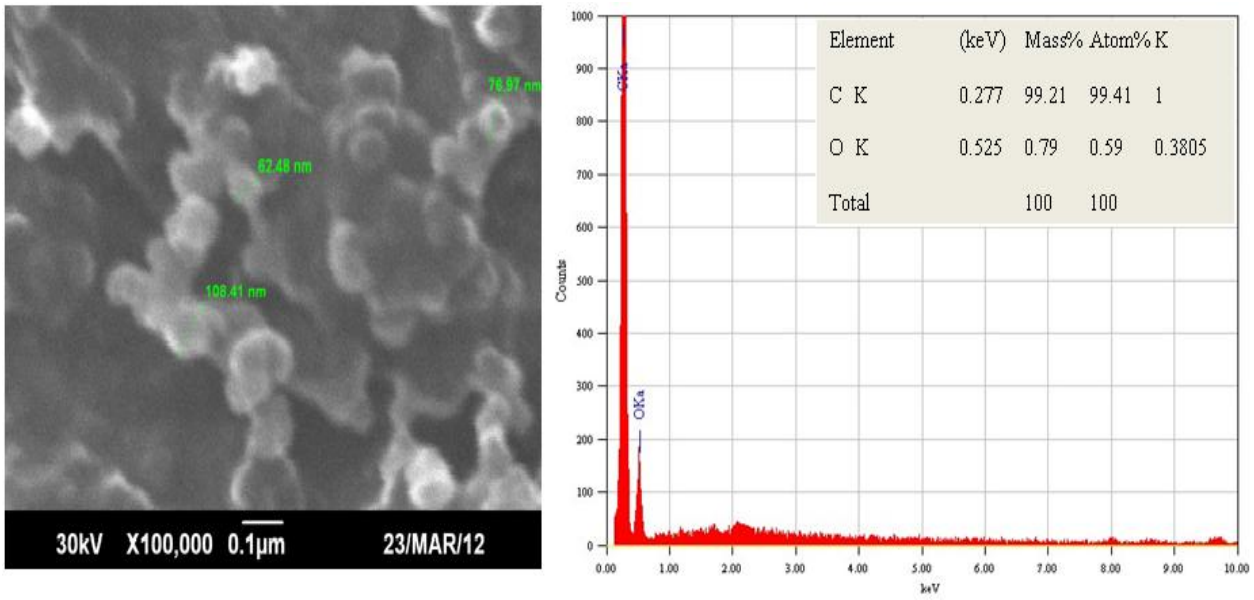

Figure 2.a. SEM-EDS analysis of soot obtained from the atmospheric combustion of kerosene

The SEM micrograph of carbon nanomaterials formed by the pyrolysis of diesel is presented in Fig.2.b. The surface morphology of the carbon nanomaterials obtained is seen to be non-uniform like kerosene soot. The micrograph looks like CNSs are formed on the surface. The particle size is found to be 48-57 nm in diameter. The composition of the diesel soot aggregates from the EDS analysis indicates that, it consists of about 97.17% weight of carbon and 2.83% weight of oxygen.

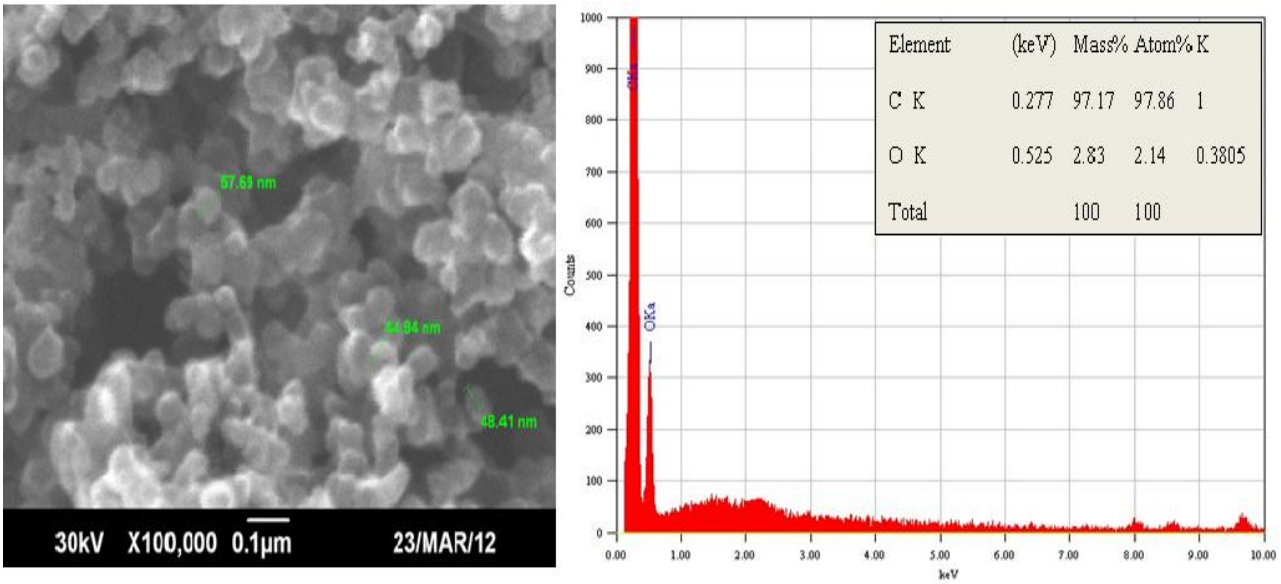

Figure 2.b. SEM-EDS analysis of soot obtained from the atmospheric combustion of diesel

From the analysis of soot obtained from paraffin wax (Fig.2.c), it is found that the nanoparticles formed has a diameter of about 80-95 nm. The EDS analysis of paraffin wax soot consists of about 96.31% weight of carbon and 3.69 % weight of oxygen.

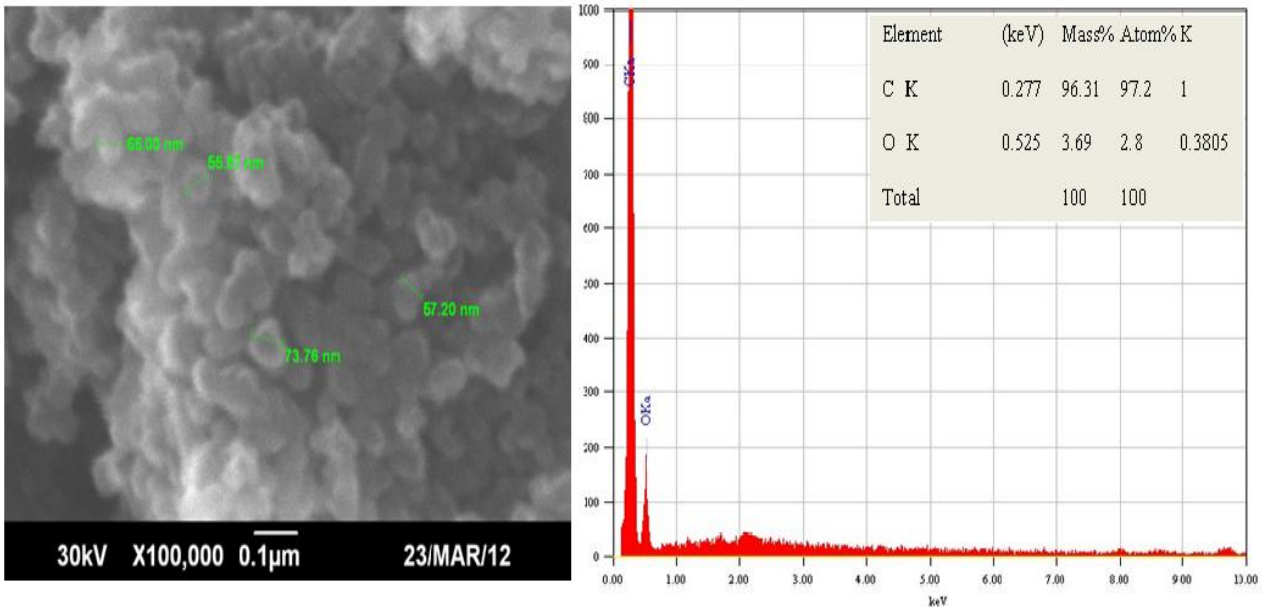

Figure 2.c. SEM-EDS analysis of soot obtained by the atmospheric combustion of Paraffin wax

The SEM image showing the morphological features of the lubricant soot under a magnification of 100,000 is shown in Fig. 2.d. The micrograph reveals the presence of non-uniform CNSs with particle size varying within the range of 45–68 nm. The EDS analysis of lubricant soot consists of about 97.4% weight of carbon and 1.06 % weight of oxygen with slight traces of Cu (1.53% weight).

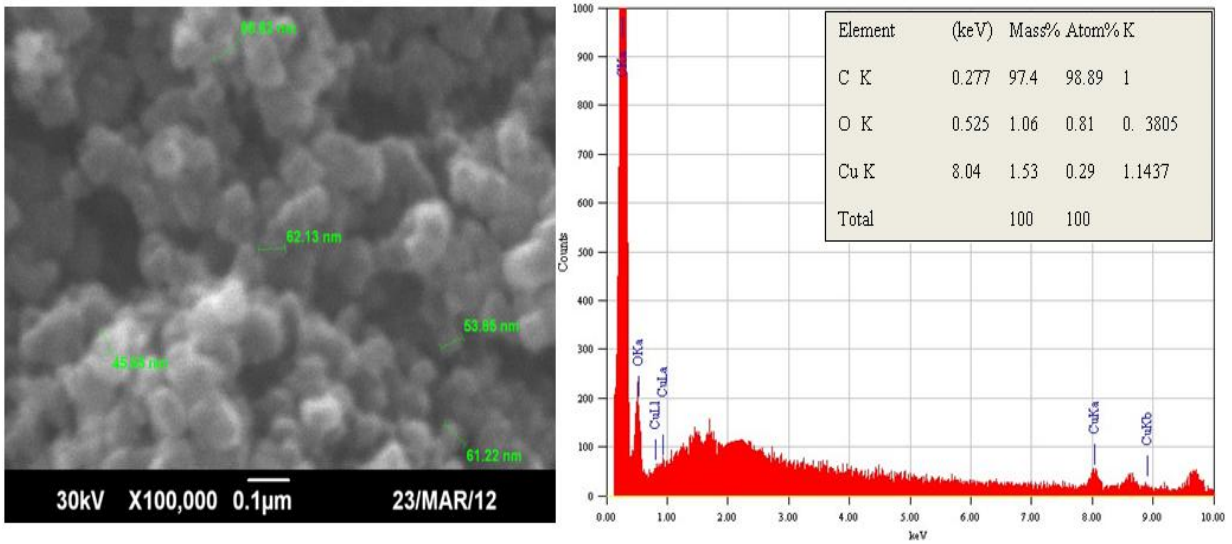

Figure 2.d. SEM-EDS analysis of soot obtained from the atmospheric combustion of lubricant

SEM images showing the topographies of non-uniform CNSs in the carbon black are presented in the Fig.2.e. The particles appear like extremely small fine grains and are found to be of the dimension 26-37 nm.

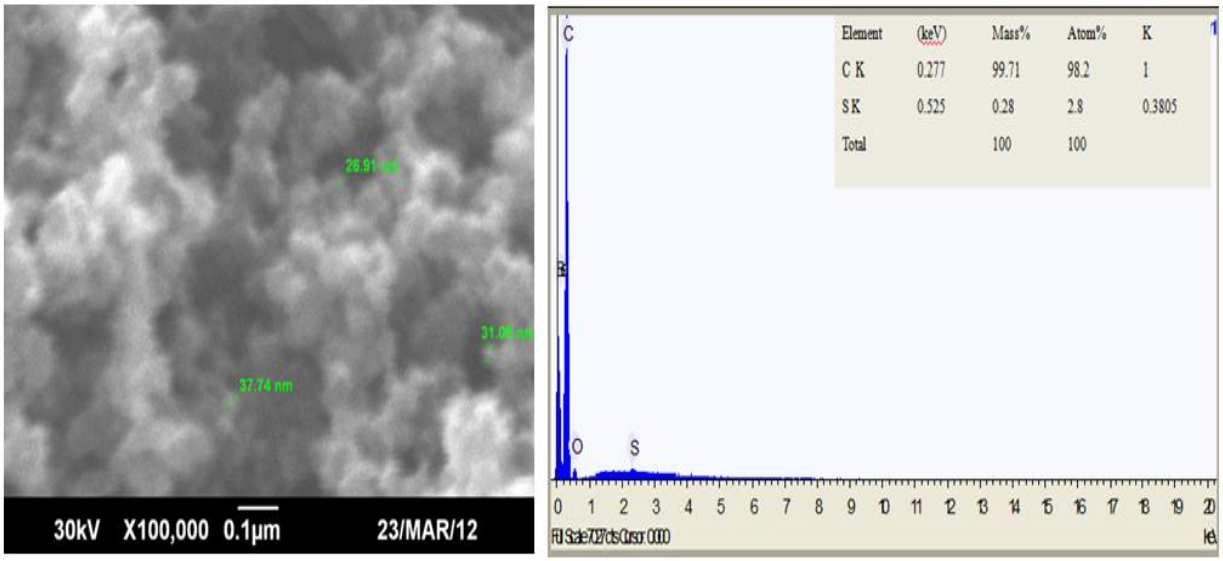

Figure 2.e. SEM-EDS analysis of the carbon black

The elemental analysis (CHNS- analysis) of the samples is presented in Table.1. Elemental carbon (C) content in the nanospheres formed by kerosene soot is found to be 99.31% weight with 0.69% weight of elemental hydrogen in it. There is absence of any other element in the sample, which support the SEM-EDS and X-ray analysis. All the three samples reveal the presence of carbon and oxygen as constituent elements without any metallic impurity in it.

The elemental analysis (CHNS- analysis) of the soot is presented in the Table.1. Elemental carbon (C) content in the nanospheres formed is found to be 99.31% weight with 0.69 % weight of elemental hydrogen in it. The absence of any other element in the sample supports the SEM-EDS and X-ray analysis. All the five samples reveal a chemical composition with more than 96% weight of carbon and admissible amounts of oxygen without any metallic impurities.

The differentiation of pure graphite from the semi-graphite can be done by the analysis of the XRD profiles and by determining the H/C ratio in the sample. The XRD analysis of the samples studied reveals a nanocrystalline, turbostratic structure. For graphite the H/C ratio ranges from 0.005-0.1 where as for semi-graphite, it varies within the limit 0.1-0.15. The H/C atomic ratio from the CHNS analysis of the investigated samples is found to be between 0.013-0.007 which confirms an ordered structure for the CNS. The H/C ratio of nanospheres formed in all the samples except paraffin wax soot is less than 0.009 and this very low value is an indication of more graphitization in the nanomaterials formed.

3.3. FTIR analysis

Infrared spectral data are used to study the carboxylic functional group of CNSs formed (Fig.3). The assignments of frequencies to their functional groups are carried out by comparison with the published work reported by various authors [12-18]. A broadened peak centred at 3442 cm^{-1} is present in all the samples, which is assigned to the (O-H) stretching vibration of the carboxylic acid

group or adsorbed water. The peaks at 2923 and 2846 cm^{-1} are assigned as CH_2 asymmetric stretching vibration and CH_3 symmetric stretching vibration respectively. The presence of the C-H stretching in aliphatic groups comes mainly from methyl, methylene and methane groups bonded to aromatic rings.

The peak observed at ~ 1630 cm^{-1} is due to the C=C stretching vibrations of graphite band (G-band) in the sample and also corresponds to the E_{2g} mode of highly oriented pyrolytic graphite. This suggests that the CNSs are composed more of crystalline graphitic carbon and the higher intensity of G-band is due to the higher degree of crystallinity/graphitization.

Kerosene soot have the highest absoprtion in the studied region. And in all the spectra, except that of lubricant soot, no peak other than graphite band is observed. Earlier studies have reported the presence of defect band (D-bnad) at 1354 cm^{-1}, which is due to the presence of asymmetric and symmetric stretching of methylene and methyl groups and this absorption band is very weak in the samples under present investigation. There is a broadening in the 1300-1000 cm^{-1} region in the spectrum of kerosene (KS). This is a complex section in the IR spectrum, where aromatic C-C and C-H plane deformation structures appear, but the most important structure corresponds to ether C-O-C stretching groups [13, 15-16].

The FTIR study reveals the presence of strong G-band with less disorder in all the samples. These results corroborate the SEM-EDS and XRD analysis. This indicates that, the degree of graphitization is maximum in kerosene soot and least in paraffin wax soot.

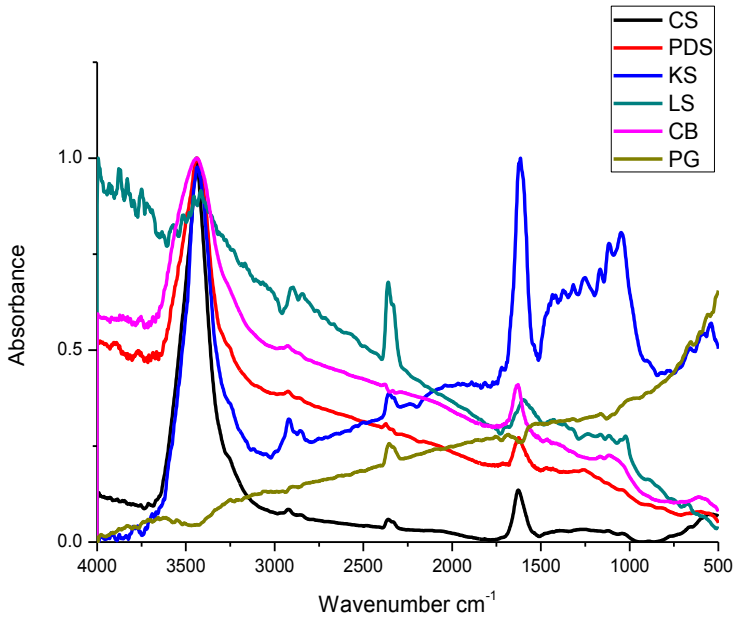

Figure 3. Infrared spectra of carbon black (CB), paraffin wax (CS), kerosene (KS), lubricant (LS), Diesel (PDS) and graphite (PG)

3.4. Micro Raman Spectroscopy

Fig.4 shows the micro-Raman spectra of grown carbon nanomaterials. In the Raman-shift range 1200-1800 cm^{-1}, two peaks are observed at ~1355 and 1602 cm^{-1} corresponding to graphite's D- and G- bands respectively. The G band corresponds to the first-order scattering of the E_{2g} mode

observed for sp^2 domains and the D band is ascribed to edge planes and disordered structures. The D band is a breathing mode associated with defects as it is forbidden in perfect single layers of graphene. The high intensity G band, assigned to the graphite phonon mode often associated with single-layer graphene, appearing in all the samples suggests the CNS is composed of crystalline graphitic carbon. The D-band, originating from the disorder in sp^2-hybridized carbon and thereby indicating the lattice distortions in curved graphene sheets and spheres etc[12-17], is very weak in the present study and is attributed to the absence of structural defects and less sp^3 –hybridized carbon. The relative intensity of these two bands (D and G peaks) which is a measure of disorder in the crystal structure is found to be very low in all the samples and hence supports the results of XRD analysis.

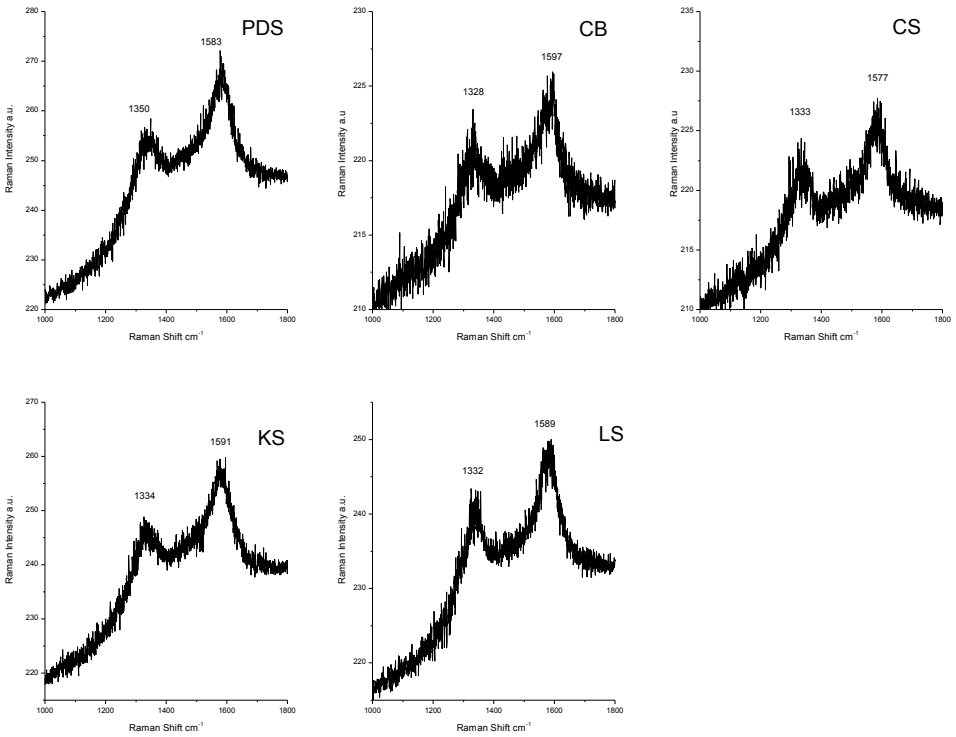

Figure 4. Micro Raman spectra carbon black (CB), paraffin wax (CS), kerosene (KS), lubricant (LS) and Diesel (PDS)

The shape of the D and G peaks depends on the crystallite sizes in the sample. When the crystallites become larger, the peak becomes narrower, their maxima move to higher frequency and the intensity of G peak (I_G) systematically increases in comparison with the D-peak (I_D). The lateral size of the crystallites are evaluated by Tuinstra and Koening relation (Equn. 1) and the values are found to be in good agreement with that calculated using the Scherrer equations (Equn.2 &3) [2,18]. The average crystallite sizes determined from both XRD and Micro Raman techniques are presented in the Table.2.

Table 2. Comparison of L_a calculated using XRD and Raman scattering

Sample	I_D/I_G	L_a (nm)by Raman	L_a (nm) by XRD
KS	0.9568	4.5464	4.7928
CS	0.9849	4.4163	4.4304
PDS	0.9513	4.5727	5.9027
LS	0.9737	4.4675	4.5518
CB	0.9887	4.3997	4.3227

I_D/I_G- D-band to G-band ratio; L_a-lateral size of the aromatic lamallae

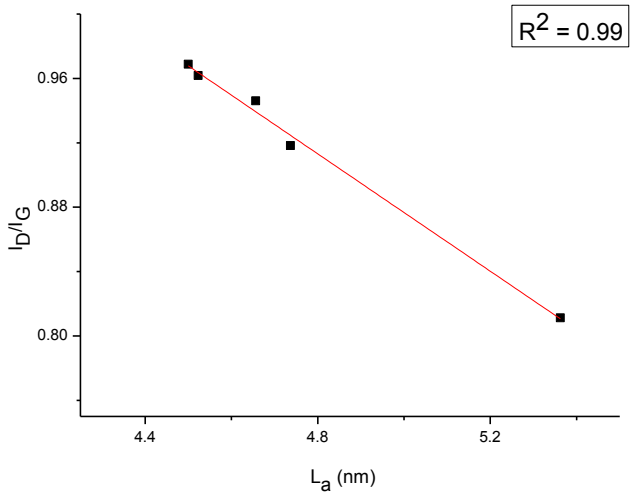

Figure 5. Plot shows I_D/I_G versus L_a

The average crystallite sizes determined by X-ray agree reasonably well with Raman except for sample KS. For these specimens Raman measurements indicate smaller crysallites than those measured by X-rays because the Raman spectra are mainly due to the outer skin of the aggregates while XRD detects crystallites throught the volume.

From the observations made throught out this study, it is infered that the nanomaterial formed from carbon black and from the pyrolysis of various hydrocarbon like kerosene, diesel, lubricant and parafiin wax are of good quality with less disordered amorphous carbon in it. The reason for getting less amorphous carbon in the deposited CNS can be explained in detail. All the samples investigated in the present study have high abundance of hexagonal and pentagonal carbon rings. During the thermal decomposition, they combine with oxygen and oxidizes the amorphous carbon present into CO_2 along with carbon soot and water vapour, which is exhausted out. The most of the CO_2 is exhausted out and its presence is confirmed by the appearence of a corresponding peak in the FT-IR spectra and the presence of water vapour was detected along the sides of the ceramic tile plate used for collecting the soot. In conventional forms of hydrocarbons like methane, ethylene etc the carbon nanostructures present results from the one-by-one addition of individual carbon atoms in the presence of a metal catalyst. In the present work the absence of any metal catalytic agent was confirmed by the EDS analysis. This suggests that the nanostructures formed here involves a slightly different

mechanism. Instead of the one-by-one addition of the individual carbon atoms, the nanostructure growth takes place by the adding up of the hexagonal and pentagonal rings as building blocks. These radicals that are in a highly active state are capable of forming a stable structure among them and in the absence of a catalyst they form stable nanospheres. In the case of soot samples, the temperature level during the combustion plays a crucial role in the formation of graphene layers. Since the retentention time of the sp^2 carbon atoms in the reaction core is not long enough to form multi-layer graphene (graphite), only few-layer graphene is kinetically favored. The most exciting feature of the nanospheres formed is that, in the optimized condition, they are free from the metallic products eliminating the need for any additional separation or purfication experiments.

4. CONCLUSION

In the present investigation it was observed that the nanomaterials formed in the samples very well obeys the Tuinstra-Koening relation. The average crystallite sizes are inversely related to the D/G intensity ratios and hence it can be concluded that all the samples contains crystalline amorphous carbon and possess a nanocrystalline structure and can be categorized as nanocrystalline graphite or the graphite-nanocrystalline graphite in the amorphization trajectory. The lateral size of the aromatic lamellae determined by using both Raman and XRD analysis are in very good agreement reinforcing the above conclusion. The high intensity Raman G band appearing at ~1630 cm^{-1} in all the spectra corresponds to the graphite phonon mode often associated with single-layer graphene and the characteristic diffraction peak of graphene is also observed in the XRD profiles. The relative intensity ratio of the γ and π bands, which is a direct indication of the quality of the carbon nanostructures formed, is found to be very low and varies from 1.1 to 0.07 thereby revealing a low amount of disorder in the CNS. The lateral size of the aromatic lamina (L_a) formed is found to be ranging from 4.3-5.9 nm where as stacking height (L_c) is found to be varying from 0.63-2.40 nm. The d_{002} spacing in all the samples is found to fall in the 3.10- 3.68 Å range which is very near to the reported interlayer spacing of the pure graphite. The topographies of the studied samples reveal the formation of CNSs with diameters falling in the range of 26-100 nm. In the IR-spectra, the graphite band is observed at ~1630 cm^{-1} which corresponds to the E_{2g} mode of highly oriented pyrolytic graphite and suggests that the CNSs are composed of crystalline graphitic carbon. EDS analysis shows that all the samples have a carbon content above ~96% and confirms the absence of any metal catalysts thereby eliminating the need for further purification methods for the nanomaterials synthesized and concludes that all the samples investigated are good and effective precursors for the formation of nanospheres possessing nanocrystalline structure and also of graphene.

ACKNOWLEDGEMENT
The authors are grateful for the support of Research and Development Cell of Christ University, Bangalore.

References

1. M.Kumar and Y. Ando, *Diamond and Related Materials*, 12 (2003)1845
2. T.Ungár, J. Gubicza, R.Gabor and Cristian Pantea, *Carbon*. 40 (2002) 929
3. D.N.Shooto and E.D. Dikio, *Int. J. Electrochem.Sci.* 6, (2011) 1269
4. E.D.Dikio, *Int.J.Electrochem.Sci.* 6 (2011)2214
5. B.Manoj and A.G.Kunjomana, *Int. J. Min. Met. and Mat*. 19(4) (2012) 279
6. B.Manoj and A.G.Kunjomana, *Int.J.Electrochem.Sci*, 7, (2012) 3127
7. B.Manoj , S.Sreelakshmi , A. N. Mohan and A.G. Kunjomana. *Int.J.Electrochem.Sci*. 7, (2012) 3215
8. B.Manoj and A.G.Kunjomana, *Trends in applied sciences research*. 7(6) (2012) 434
9. B.Manoj and A.G. Kunjomana, *J. Min. Mat.Ch. and Eng*. 9 (10) (2010) 919
10. B.Manoj and A.G.Kunjomana A.G, *Asian Journal of Material Science*. 2(4), (2010)204
11. O.O.Sonibare, T. Haeger, and S.F. Foley, *Energy.* 35 (2010) 5347
12. A.Santamaria , F. Mondragon, A. Molina, N.D. Marsh, E.G. EEddings and A.F. Sarofim, *Combustion and flame*.146 (2006) 52
13. A.Santamaria, N.Yang, F.Mondragon and E.G.Eddings. *Combustion and flame*. 157, (2010)33
14. A.C.Ferrari and J. Robertson, *Physical Review* B. 61(20), (2000)14095
15. A. Chakrabarti, J.Lu, J.C.Skrabutenas, T.Xu, Z. Xiao, J.A.Maguire and N.S. Hosmane, *J.Mater.Chem*. 21 (2011) 9491
16. A.Ilyin, N. Guseinon, A. Niktin and I. Tsyganov ,*Physica* E. 42(8) (2010) 2078
17. P. Dubey, D.Muthukumar, S.Dash, R.Mukopadhyay and S. Sarkar, *Pramana Journal of physics*. 65(4) (2005)681
18. F.Tuinstra and J.L.Koening *J.Chem.Phys*. 53 (1970)1126